Anisotropy Decay Measurement of Segmental Dynamics of the Anion Binding Domain in Erythrocyte Band 3†

S. Bicknese, Mary Rossi, B. Thevenin, S. B. Shohet, and A. S. Verkman*

Departments of Medicine and Physiology, Cardiovascular Research Institute and Department of Laboratory Medicine, University of California, San Francisco, California 94143-0521

Received March 3, 1995; Revised Manuscript Received May 31, 1995®

ABSTRACT: Time-resolved anisotropy was utilized to detect nanosecond segmental motions of the band 3 intramembrane domain. Band 3 at lysine 430 was fluorescently labeled in ghost membranes by fluorescein or eosin maleimide treatment of intact human erythrocytes followed by hypotonic lysis. Single lifetimes for fluorescein (3.8−4.1 ns) and eosin (3.2−3.4 ns) were observed. Phase-modulation measurement of anisotropy decay indicated a segmental motion model, $r(t) = \exp(-t/\tau_{1c})[r_\infty + (r_0 - r_\infty)\exp(-t/\tau_{2c})]$, defined by rotational correlation times corresponding to band 3 segmental motion (τ_{1c}, 30−70 ns) and rapid fluorescein motion in its binding pocket (τ_{2c}, 200−400 ps), and a residual anisotropy (r_∞, 0.23−0.28) describing hindered fluorescein motion. In PBS at pH 7.4, τ_{1c}, τ_{2c}, and r_∞ were 44 ns, 307 ps, and 0.24, respectively, predicting a steady-state anisotropy of 0.24, in agreement with the measured value of 0.23. Factors that might influence band 3 structure/dynamics were examined. Whereas pH (range 5−10) had little effect on $r(t)$, [NaCl] addition (0−150 mM) remarkably decreased τ_{1c} from 68 to 44 ns. The decrease in τ_{1c} correlated with solution ionic strength, and did not depend on osmolality (studied by mannitol addition), or specific anion interactions (comparing Cl, Br, F, SO_4, citrate). The ionic strength effect was not observed in fluorescein-labeled carbonic anhydrase and trypsin-cleaved band 3, suggesting a specific effect on intact band 3. Anisotropy decay was relatively insensitive to external lectin or internal 2,3-DPG binding, but was sensitive to temperature, membrane fluidity, urea denaturation, fluid-phase viscosity, and aldehyde fixation. These studies provide the first data on the nanosecond segmental dynamics of the intramembrane domain of band 3 and revealed an unexpected sensitivity to solution ionic strength.

Band 3 is the major anion exchange protein of human erythrocytes and provides an important anchorage site linking the plasma membrane with the underlying skeleton [for review, see Jennings (1989), Reithmeier (1993), Tanner (1993), and Wang (1994)]. Band 3 is assembled as dimers in membranes in which monomers interact allosterically (Verkman et al., 1983; Salhany, 1990; Casey & Reithmeier, 1991). Recent low-resolution (2 nm) studies by electron crystallography revealed that each dimer is a U-shaped structure with a deep depression or "canyon" facing the external surface (Wang et al., 1994). On the basis of the fluorescence quenching and energy transfer studies, it has been proposed that the external anion binding site is located in a deep cavity within band 3 and that rapid anion exchange may involve the movement of a thin permeability barrier near the internal membrane surface (Passow, 1983; Jennings, 1989; Wang, 1994). Because chloride−bicarbonate exchange occurs at an exceptionally high turnover rate ($\sim 10^5$ s^{-1}), the anion binding domain is expected to undergo dynamic segmental motions on the nanosecond-to-microsecond time scales. Although there are extensive data on anion exchange kinetics (Jennings, 1989; Salhany, 1990), translational and rotational motions of the whole band 3 molecule (Nigg & Cherry, 1980), and kinetics of stilbene-induced band 3 conformational changes (Verkman et al., 1983; Salhany et al., 1993), there is no information about the nanosecond segmental dynamics of the intramembrane domain of band 3.

Time-resolved fluorescence anisotropy provides quantitative information about fluorophore rotation on the time scale of tens of picoseconds to hundreds of nanoseconds. For a fluorophore bound to a specific site on a soluble or membrane protein, time-resolved anisotropy measurements give the rate and extent of fluorophore rotation in its binding pocket, as well as the rate and extent of local protein segmental motions. In erythrocytes, time-resolved anisotropy has been utilized recently to study microsecond motions of fluorescently-labeled spectrin (Clague et al., 1990), and nanosecond motions of the cytoplasmic domain of band 3 (cdb3) (Thevenin et al., 1994). In the latter study, analysis of fluorescein rotation at residue cysteine 201 at the "hinge" region of cdb3 revealed rapid fluorescein rotation in its binding pocket (~100 ps) and slower cdb3 segmental motion (~4 ns). Both motions were hindered; the extent of cdb3 segmental motion was strongly dependent on pH and was influenced by agents which bind to cdb3, including 2,3-DPG and several glycolytic enzymes.

The purpose of this study was to quantify nanosecond segmental motions of the intramembrane domain of band 3, and to determine whether this motion was sensitive to putative modulators of band 3 structure/function. Time-resolved anisotropy was measured in erythrocyte ghost membranes in which the intramembrane domain of band 3

† This work was supported by Grants DK43840 and DK16095 from the National Institutes of Health.

* Address correspondence to this author at the Cardiovascular Research Institute, University of California, 1246 Health Sciences East Tower, San Francisco, CA 94143-0521. Phone: (415)-476-8530. Fax: (415)-665-3847.

® Abstract published in *Advance ACS Abstracts,* August 1, 1995.

0006-2960/95/0434-10645$09.00/0

was fluorescently labeled. An ~40 ns rotational correlation time corresponding to band 3 segmental motion was detected at physiological ionic strength, as well as rapid (~300 ps) hindered rotation of fluorescein in its binding pocket. Band 3 motion was not sensitive to pH or to agents which interact with external sugars or internal cdb3, but was sensitive to solution ionic strength and to several factors which influence the physical environment in the vicinity of band 3.

METHODS

Membrane Preparation and Labeling. Freshly drawn red cells from healthy adult volunteers were washed 3 times in 25 mM sodium phosphate, 1 mM EDTA, and 95 mM NaCl (pH 7.4, buffer A) and suspended at 50% hematocrit. FM (fluorescein-5-maleimide; Molecular Probes, Eugene, OR) in DMF (150 mM) was added to the cell suspension at a final concentration of 1 mM while vortexing. The reaction was terminated after 2 h at 23 °C by 10-fold dilution into 1 mM cysteine, 5 mg/mL BSA in buffer A. The fluorescein-labeled cells were then washed 4 times in PBS, lysed in 5 mM sodium phosphate, 1 mM EDTA, pH 8.0 (lysis buffer), and washed until the supernatant was colorless. Fluorescein-labeled ghosts were stored on ice until use. Eosin-labeled ghosts were prepared by the same protocol, except that eosin maleimide (Molecular Probes) was substituted for FM. Fluorescein-labeled carbonic anhydrase was prepared by reaction of carbonic anhydrase (10 mg/mL, Sigma) in buffer A with 7.5 mM FM for 2 h at 23 °C, followed by extensive dialysis against lysis buffer. For trypsin cleavage of the membrane domain of band 3, fluorescein-labeled ghosts at 1 mg of protein/mL in lysis buffer were incubated for 30 min at 4 °C with 0.2 mg/mL trypsin (TPCK-treated, Cooper Biomedical). The reaction was stopped with 1 mM diisopropyl fluorophosphate and centrifuged twice (30000*g*, 10 min) to remove the band 3 cytoplasmic domain. Samples were electrophoresed on 8.5% Laemmli polyacrylamide gels and stained with Coomassie blue. Protein was assayed by the standard Lowry method. Labeling stoichiometry was calculated from protein concentration and sample absorbance using molar extinction coefficients of 83 000 M^{-1} cm^{-1} (fluorescein) and 100 000 M^{-1} cm^{-1} (eosin) and assuming that band 3 comprised 25% of membrane protein.

Sample Preparation for Anisotropy Measurements. Fluorescein-labeled ghosts were suspended in specified buffers at 60 μg of protein/mL in duplicate and equilibrated overnight at 4 °C. All buffers (except for the "zero" osmolality buffer) contained 1 mM sodium phosphate and were titrated to specified pH with HCl or NaOH. A 2 mM octanol solution was prepared by injection of a 10% stock solution of octanol in ethanol into PBS while vigorously vortexing. Wheat germ agglutinin (Sigma) samples were prepared by addition of 50 μg of WGA to the ghost suspension immediately before experiments. No agglutination was observed under these conditions. Solution osmolalities were measured on a Wescor 5100C Osmometer (Logan, UT), and ionic strengths were deduced from the CRC Handbook.

Steady-State Fluorescence Measurements. Fluorescence spectra were measured on an SLM 8000c fluorometer (Urbana, IL). Corrected spectra were utilized for quantum yield determinations. Steady-state anisotropy measurements on fluorescein-labeled ghosts (62 μg of protein/mL) were carried out on an SLM 48000MHF fluorometer with vertically-polarized Ar laser excitation (488 nm) and photomultiplier detection using a 515 nm cut-on filter and rotatable analyzing polarizer. All measurements were made in triplicate. Dilution controls were carried out to ensure that anisotropy values were not affected by scattering or other concentration-dependent artifacts.

Measurement of Time-Resolved Fluorescence. Fluorescence lifetimes and anisotropy decay were measured by parallel acquisition frequency-domain fluorometry on a Fourier transform SLM 48000MHF fluorometer (Fushimi & Verkman, 1991). Samples in cuvettes (quartz, 2 × 10 mm) were excited with vertically-polarized impulse-modulated light from an Ar laser (Coherent; 488 nm). Lifetime measurements were made with fluorescein in 0.1 N NaOH (4.0 ns) as reference. The emission path contained a 515 nm cut-on filter (OG515, Schott Glass) and a Glan-Thompson polarizer oriented at the magic angle. Phase and modulation values (5−200 MHz) were fitted to single- or double-component lifetime decays using SLM software. Anisotropy decay measurements were performed by comparing parallel and perpendicular orientations of the emission polarizer (Lakowicz et al., 1993). Each sample (prepared in duplicate) was measured twice; each individual measurement was the median value of 4−6 paired (parallel and perpendicular polarizer orientations) 15 s data accumulations. Multifrequency differential phase angles and modulation amplitude ratios (6−204 MHz) were fitted by nonlinear regression (Calafut et al., 1989) to multicomponent anisotropy decay [$r(t)$] models (see Results) or to the segmental motion model:

$$r(t) = \exp(-t/\tau_{1c})[r_\infty + (r_o - r_\infty)\exp(-t/\tau_{2c})] \quad (1)$$

where r_o is the limiting anisotropy in the absence of depolarizing rotations (0.392 for fluorescein), τ_{1c} and τ_{2c} are rotational correlation times of slower (segmental motion) and faster (rotation in binding pocket) fluorophore motions, respectively, and r_∞ is the residual anisotropy corresponding to hindered fluorophore rotation in its binding pocket. Background signal (unlabeled sample) was <1% of sample fluorescence. Dilution controls were carried out to show that fitted lifetimes and anisotropy decay parameters were insensitive to sample concentration. No photobleaching occurred under the conditions of the experiment, and fitted results were stable in serial measurements performed over 1 h in a single sample.

RESULTS

Figure 1 (lanes a−d) shows the fluorescence labeling of erythrocyte band 3. To maximize labeling specificity, reactions were carried out in intact erythrocytes from which unsealed ghost membranes were prepared by hypotonic lysis. The major protein labeled by fluorescein maleimide was band 3 (lane a). Trypsin cleavage produced a single labeled band corresponding to the 17 kDa (residues Gly 361 to Tyr 553; Lux et al., 1989) membrane-associated fragment of the intramembrane domain of band 3 (lane b) (Macara et al., 1983). The cytoplasmic domain of band 3 was not labeled. Lane c shows specific band 3 labeling with eosin maleimide. The molar labeling stoichiometry (mol:mol, fluorophore:band 3 monomer), as determined by absorbance and protein assays, was 0.54 for fluorescein and 0.90 for eosin. Greater than 90% of each fluorescent label was associated with band 3

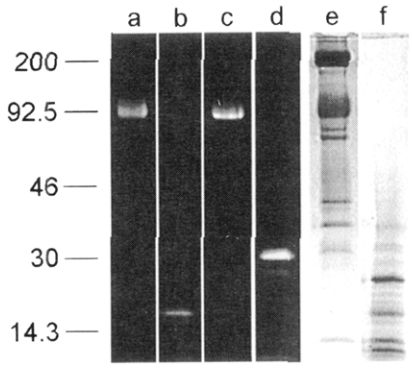

FIGURE 1: Fluorescence labeling of the intramembrane domain of erythrocyte band 3 in unsealed ghosts. SDS−PAGE showing fluorescence (lanes a−d) and Coomassie blue staining (lanes e, f). Samples consisted of erythrocyte ghost proteins labeled with fluorescein maleimide before (lanes a, e) and after (lanes b, f) trypsin cleavage, ghost membrane proteins labeled with eosin maleimide (lane c), and carbonic anhydrase labeled with fluorescein maleimide (lane d).

as judged by quantitative fluorescence imaging of the gels. Labeling of the 17 kDa fragment (fluorescein, lane b; eosin, not shown) is in agreement with previous data showing selective eosin maleimide labeling of residue lysine 430 (Cobb & Beth, 1990). Fluorescence spectra for fluorescein- and eosin-labeled band 3 in intact erythrocyte ghosts showed excitation/emission maxima at 492/524 nm (fluorescein) and 530/555 (eosin). Anisotropy measurements were carried out at excitation/emission wavelengths of 488/>515 nm. The fluorescence quantum yield of fluorescein bound to band 3 was 0.69 as determined by integration of the corrected emission spectra using fluorescein in 0.1 M NaOH as a reference. Lane d contains fluorescein-labeled carbonic anhydrase, a 30 kDa protein having a single cysteine residue.

Time-resolved measurements of fluorescence lifetime and anisotropy were carried out by phase-modulation fluorometry (Figure 2). Phase-modulation data for lifetime measurements in fluorescein- and eosin-labeled ghosts fitted well to single-component lifetimes of 3.9 and 3.2 ns, respectively, in PBS at pH 8.0, 23 °C (Figure 2A,B). There was under 5% contribution from a second lifetime component. The fluorescein lifetime varied by less than 0.3 ns for the various experimental conditions described below. The corresponding phase-modulation data for anisotropy decay (for the same sample) did not fit adequately to a single-component decay (dashed curves, Figure 2C) or a single-component-hindered rotational model (dotted curves), but did fit well to a segmental motion model containing rotational correlation times corresponding to relatively slow segmental motions of band 3 in the region of the anion binding site (τ_{1c}, ~40 ns) and rapid fluorescein rotation in its "binding pocket" (τ_{2c}, ~300 ps) (see Figure 2D for residuals plot). A third parameter (residual anisotropy, r_∞) quantified the "hindrance" to fluorescein rotation in its binding pocket; an r_∞ of 0.24 measured here corresponded to fluorophore rotation in an effective cone of angle ~38°. Data regression utilizing more complex anisotropy decay models, including a three-exponential anisotropy decay model, and a segmental model in which both rapid and slower fluorescein motions were hindered, indicated that $r(t)$ in eq 1 was adequate to describe the data for the studies reported below. Reduced χ^2 was generally in the range 0.8−1.5; regression of phase-modulation data to a three-component anisotropy decay model returned a fractional amplitude for the third component (corresponding to very slow rotation) of under 5%. Figure 2E shows qualitative differences in differential phase angles and modulation amplitude ratios when the same experiment was carried out in the absence of NaCl ("0 mM NaCl") instead of PBS (150 mM NaCl). It was found that citrate (Figure 2F), but not mannitol (Figure 2G), could reproduce the effect of NaCl (see below for fitted results). Figure 2H shows that partial protein denaturation by 8 M urea caused a marked change in phase and modulation values.

The hypothesis was next tested that certain physical and chemical factors believed to influence band 3 structure affect segmental dynamics in the intramembrane domain of band 3. Solution pH has been shown to modulate band 3 anion exchange rates for monovalent and divalent anions (Jennings, 1989), and to dramatically alter the configuration of the cytoplasmic domain of band 3 (cdb3) (Low et al., 1988). Figure 3A shows the minor influence of pH on the parameters τ_{1c}, τ_{2c}, and r_∞ in the range 7−10. The results sharply contrast with a previous study of segmental motions at the "hinge region" (Cys 201) of cdb3 (Thevenin et al., 1994), in which the parameters describing cdb3 segmental motion were strongly influenced by pH in the range 8−9.5. The present results suggest that substantial changes in the conformation of cdb3 had little effect on segmental motions in the intramembrane domain of band 3, consistent with the observation that cdb3 cleavage does not alter anion exchange kinetics (Lepke et al., 1992).

Significant pH effects on anion exchange (Jennings, 1989) and possibly band 3 structure (Yamakose et al., 1993) occur in the pH range 4−7. Studies with the fluorescein-labeled sample could not be carried out below pH 7 because the fluorescein chromophore becomes protonated and non-fluorescent. Anisotropy decay measurements in the pH range 4−8 were therefore carried out for eosin-labeled band 3 sample. All eosin samples had a single fluorescence lifetime in the range 3.2−3.4 ns. There was no significant effect of pH in the range 5−8, where phase-modulation data fitted well to the segmental motion (eq 1), with τ_{1c} of 110−130 ns, τ_{2c} of 650−700 ps, and r_∞ of 0.23−0.28. However, at pH 4, τ_{1c}, τ_{2c} and r_∞ were 55 ± 9 ns, 452 ± 12 ps, and 0.26 ± 0.01, respectively (SE, $n = 4$). This remarkable change in eosin rotation between pH 5 and 4 probably corresponds to an effective "pK_a" of 4.3 deduced from eosin-labeled band 3 spectral properties (Yamakose et al., 1993), which was proposed to represent pH-dependent electrostatic interactions between eosin and band 3.

The influence of NaCl concentration on band 3 segmental dynamics was next examined (Figure 3B). There was a remarkable decrease in τ_{1c} for the fluorescein-labeled sample with increasing [NaCl], corresponding to an increased rate of band 3 segmental motion. The effect was nearly maximal at 6 mM NaCl. There was a smaller though significant change in the parameters τ_{2c} and r_∞, suggesting that rapid fluorescein motion in its binding pocket becomes slower and less hindered with increasing [NaCl] in the range 0−4 mM. The fluorescein lifetime (τ_f) varied little (from 4.0 to 3.9 ns) as [NaCl] increased from 0 to 150 mM (not shown). Steady-state fluorescence anisotropy (r_{ss}) was calculated from τ_{1c}, τ_{2c}, and r_∞ from the relation $r_{ss} = r_\infty/(1 + \tau_f/\tau_{1c}) + (r_o - r_\infty)/(1 + \tau_f/\tau_{2c})$. Computed r_{ss} was predicted to decrease from 0.27 to 0.23 with increasing [NaCl] (0−150 mM). Measured r_{ss} values decreased from 0.26 to 0.24 (0−150

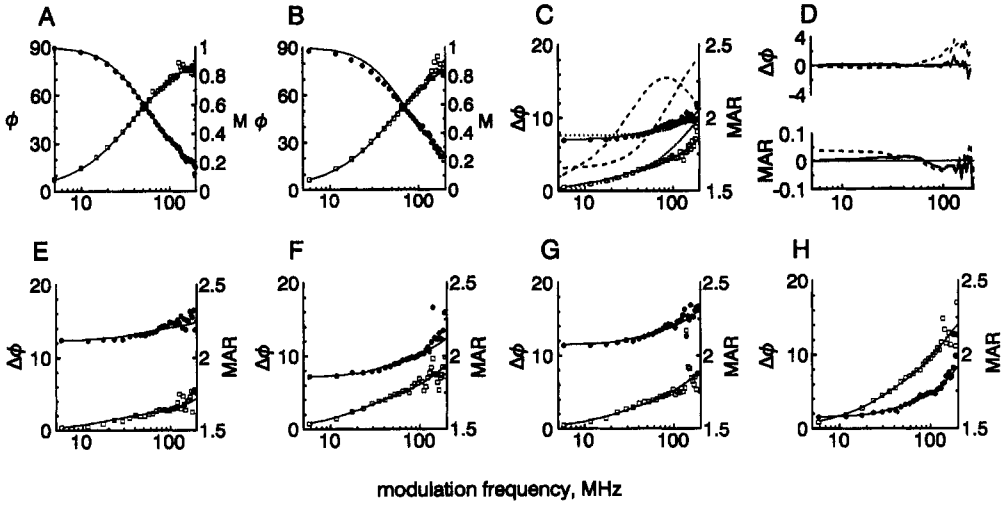

FIGURE 2: Time-resolved fluorescence measurements of the fluorescein-labeled intramembrane domain of band 3 in ghost membranes. (A and B) Phase angles (ϕ, open squares) and modulation ratios (M, filled circles) for fluorescein-labeled ghosts (A) and eosin-labeled ghosts (B) in PBS. Fitted fluorescence lifetimes were 3.9 and 3.2 ns, respectively (solid lines). (C) Differential phase angles ($\Delta\phi$, open squares) and modulation amplitude ratios (MAR, filled circles) for anisotropy measurement in the same sample. Data were fitted to a single-component rotation model (dashed curves, $\chi^2 = 245$), a single-component hindered rotator model (dotted curves, $\chi^2 = 5.2$), and a segmental motion model (eq 1, solid curves, $\chi^2 = 0.8$). (D) Residuals plot corresponding to the data in (C) for the single-component hindered rotation model (dashed curves) and the segmental motion model (solid curves). (E–H) Anisotropy studies of fluorescein-labeled ghosts at low osmolality (0 mM NaCl, panel E), citrate (25 mM, panel F), mannitol (290 mM, panel G), and urea (8 M, panel H). See Methods for details. Fitted rotational parameters are summarized in Figures 3 and 4.

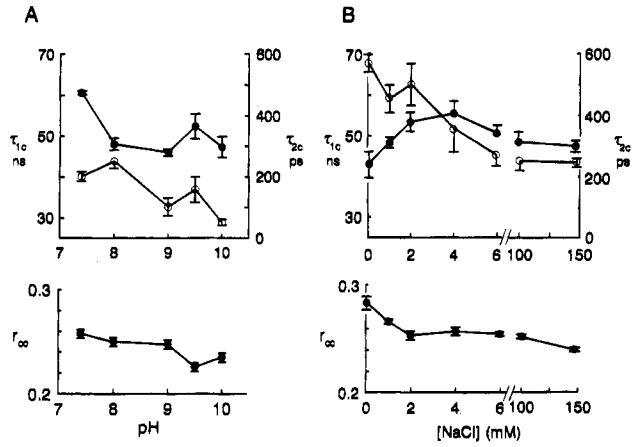

FIGURE 3: Influence of pH (A) and [NaCl] (B) on time-resolved anisotropy of fluorescein-labeled band 3 in ghost membranes. Phase and modulation values were fitted to the segmental motion model in eq 1. Data are shown as mean and SE for measurements performed at 23 °C in quadruplicate (pH studies) and 8–16 times in 4 separate sets of measurements (NaCl studies).

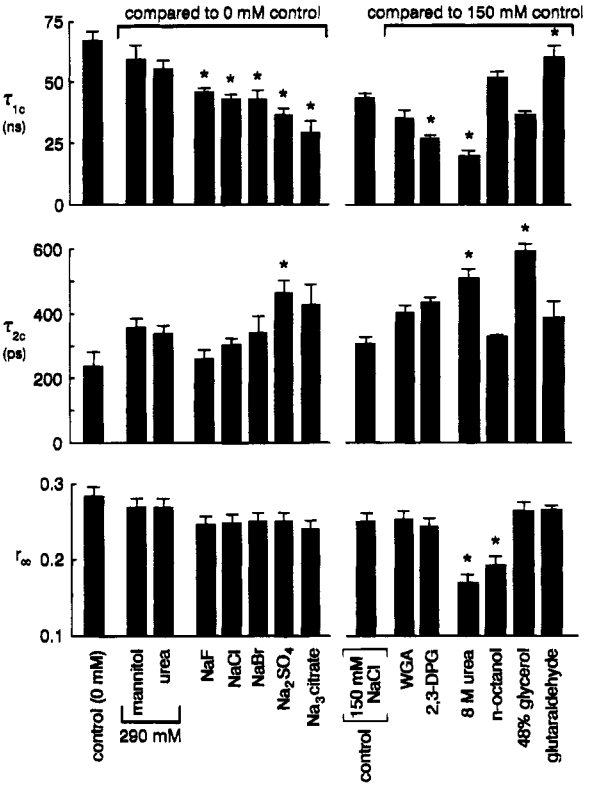

FIGURE 4: Effects of putative modulators of band 3 structure on time-resolved anisotropy of the fluorescein-labeled intramembrane domain of band 3. Measurements were carried out at 23 °C. Fitted parameters (mean ± SE, $n = 4$–30) for the segmental motion model were obtained from phase-modulation data by nonlinear regression using eq 1. Concentrations were as follows: mannitol and urea, 290 mM; NaCl, NaF and NaBr, 150 mM; Na_2SO_4, 55 mM; Na citrate, 25 mM; WGA, 50 μg/mL; 2,3-DPG, 20 mM; octanol, 2 mM; and gluteraldehyde, 0.1%. An asterisk denotes significant difference compared to the indicated control ($p < 0.01$).

mM), in agreement with r_{ss} calculated from parameters of the anisotropy decay model. This good agreement between measured and calculated r_{ss} is not often observed, and strongly supports the conclusion that the segmental motion model utilized here is adequate to describe the fluorescein–band 3 rotational data.

The sensitivity of fluorescein–band 3 anisotropy decay to [NaCl] could be a consequence of changes in osmolality, ionic strength, and/or interactions of specific anions. Figure 4 shows that increasing solution osmolality with the uncharged solutes mannitol or urea (290 mM) (in place of NaCl) did not reproduce the effect of NaCl. (290 mM urea does not cause band 3 denaturation.) To investigate whether the [NaCl] effect was specific for chloride, experiments were carried out with fluoride, bromide, sulfate, and citrate. Each of these ions decreased τ_{1c}. Because the interaction of sulfate with the anion binding site is different from that of chloride, and because citrate interacts only weakly with the anion

Table 1: Influence of Ionic Strength on Anisotropy Decay in Trypsin-Cleaved Band 3 and Carbonic Anhydrase[a]

[NaCl] (mM)	τ_{1c} (ns)	τ_{2c} (ps)	r_∞
	Trypsin-Cleaved Band 3		
0	37 ± 3	401 ± 18	0.22 ± 0.01
2	34 ± 4	405 ± 30	0.20 ± 0.01
4	27 ± 1	404 ± 20	0.19 ± 0.01
6	31 ± 4	428 ± 25	0.18 ± 0.01
150	30 ± 3	370 ± 21	0.17 ± 0.01
	Carbonic Anhydrase		
0	6.5 ± 0.2	241 ± 22	0.21 ± 0.01
2	6.7 ± 0.3	240 ± 15	0.21 ± 0.01
4	6.7 ± 0.2	233 ± 12	0.20 ± 0.01
6	8.1 ± 0.9	261 ± 35	0.19 ± 0.01
150	6.5 ± 0.6	191 ± 25	0.21 ± 0.01

[a] Samples contained fluorescein-labeled band 3 in ghosts after trypsin cleavage (62 μg of protein/mL) and fluorescein-labeled carbonic anhydrase (30 μg/mL). Fitted parameters (mean + SE, 4−6 experiments) for anisotropy decay (eq 1) are given. Measurements were carried out at pH 8.0, 23 °C, in buffers containing 1 mM sodium phosphate and the indicated [NaCl].

binding site (K_d 125 mM; Schnell et al., 1978), these results indicate that specific anion interactions at the anion binding site do not account for the NaCl effect on band 3 segmental motion. The best correlation of τ_{1c} was with ionic strength; for the mono-, di-, and trivalent anions chloride, sulfate, and citrate, solutions of approximately equal ionic strength caused comparable decreases in τ_{1c}. A correlation with Debye length (inversely proportional to [ionic strength]$^{1/2}$) is suggested based on the concentration dependence in Figure 1B showing the main effect at low [NaCl]. The Debye length, which decreases from 9.6 to 0.8 nm as ionic strength increases from 1 to 150 mM, was significantly correlated with τ_{1c} ($r = 0.86$, linear correlation coefficient).

To determine whether this apparent ionic strength effect was specific for intact band 3, experiments were carried out with trypsin-cleaved band 3 and fluorescein-labeled carbonic anhydrase, a 30 kDa soluble protein having a single cysteine residue (Table 1). Trypsin cleavage was carried out under conditions which caused release of the cytoplasmic domain of band 3, as well as intramembrane cleavage (Macara et al., 1983; see Figure 1). The remaining fluorescein-labeled ~17 kDa fragment of band 3 remained membrane-associated under the cleavage and washing conditions. Although trypsin cleavage caused a remarkable change in anisotropy decay parameters, there was no significant effect of [NaCl] on these parameters. Similarly, there was little effect of [NaCl] on the anisotropy decay of FITC-labeled carbonic anhydrase. Taken together, these results suggest that ionic strength influences band 3 segmental motion in a manner that requires an intact transporter.

Several compounds that interact with band 3 were examined (Figure 4). Addition of wheat germ agglutinin, a lectin which binds to the external sugar moiety of band 3, did not significantly affect anisotropy decay. Binding of 2,3-DPG to the cytoplasmic domain of band 3 had a relatively small effect on anisotropy decay. In previous studies, binding of 2,3-DPG under these conditions influenced significantly the segmental motion of cdb3 (Thevenin et al., 1994). Partial denaturation of band 3 by 8 M urea remarkably altered fluorescein rotation, resulting in more rapid segmental motion, and less hindered but slower fluorescein motion in its binding pocket. Increasing erythrocyte membrane "fluidity" by 1-octanol also decreased the hindrance to fluorescein rotation, consistent with the observation that various membrane-fluidizing agents, including a series of 1-alkanols, increased the kinetics of band 3 conformational change induced by stilbene binding (Forman et al., 1984). To test whether external solution microviscosity affected fluorescein rotation, the small molecule glycerol was added. In contrast to the effect observed for 1-octanol, glycerol caused a selective increase in the parameter τ_{2c}, corresponding to slowed fluorescein rotation in its binding pocket. Taken together, these results support the assignment of τ_{2c} as rapid fluorescein rotation in its binding pocket and τ_{1c} as slower band 3 segmental motion. Finally, as expected, partial cross-linking of erythrocyte membrane proteins by 0.1% glutaraldehyde caused a remarkable decrease in the rate of band 3 segmental motion.

Temperature dependence studies were carried out to further characterize the intramembrane band 3 segmental motion. Brahm (1977) reported a 20 kcal/mol activation energy for anion exchange above 15 °C and a higher activation energy at lower temperatures. For fluorescein-labeled ghosts, fitted (τ_{1c}, τ_{2c}, and r_∞) values were 78 ns, 297 ps, 0.21 (10 °C, 0 mM NaCl); 29 ns, 229 ps, 0.21 (10 °C, 150 mM NaCl); 68 ns, 222 ps, 0.19 (34 °C, 0 mM NaCl) and 33 ns, 155 ps, 0.18 (34 °C, 150 mM NaCl). Interestingly, the segmental motion (τ_{1c}) was slowed with increasing temperature at 150 mM NaCl, but accelerated at 0 mM NaCl. At both ionic strengths, the rate of fluorescein rotation in its binding pocket (τ_{2c}) was increased with increasing temperature. These complex effects of temperature are difficult to interpret because of multiple temperature-dependent processes, including solution and membrane viscosity, anion binding, and molecular diffusion.

DISCUSSION

The purpose of this study was to utilize time-resolved fluorescence anisotropy to characterize rapid segmental motions of the intramembrane domain of band 3, the region of band 3 involved in anion exchange. Erythrocyte band 3 contains an amino-terminal cytoplasmic domain (43 kDa, residues 1−360) and a carboxy-terminal intramembrane domain (52 kDa, residues 361−911) that probably spans the membrane 14 times (Kopito & Lodish, 1985; Wang, 1994). Selective fluorescence labeling of the intramembrane domain was accomplished with fluorescein and eosin chromophores, and multicomponent anisotropy decays were resolved in intact membrane samples. Time-resolved anisotropy of fluorescein-labeled band 3 revealed two distinct rotational components: a fast rotation (200−400 ps) that was significantly hindered (residual anisotropy 0.23−0.28) and a slower rotation (30−70 ns). The rotational model and parameters differed from data for the fluorescein-labeled cytoplasmic domain of band 3, where fast (~100 ps) and slower (~4 ns) hindered rotations were detected (Thevenin et al., 1994). The fast rotation here corresponded to hindered fluorescein rotation in its binding pocket, and the slower rotation corresponded to a segmental motion of the intramembrane domain of band 3. Both motions were sensitive to several putative modulators of band 3 structure.

Cobb and Beth (1990) showed that erythrocyte band 3 was labeled selectively by eosin maleimide at lysine 430 under the reaction conditions utilized here. Proteolysis and solubilization in SDS produced a single labeled 17 kDa fragment

derived from the intramembrane domain of band 3, similar to our results for labeling with fluorescein and eosin maleimide. It is noted that the single "cryptic" cysteine residue at position 479, which does not react with *N*-ethylmaleimide (Rao & Reithmeier, 1979), was not labeled. Because the atomic resolution structure of band 3 is not known and the anion binding site has not been resolved, the physical location of the fluorescently-labeled site on band 3 cannot be specified. Hydropathy analysis suggests that lysine 430 is located near the extracellular membrane surface in a domain connecting the first and second membrane-spanning segments of band 3. Proximity to the "anion transport site" is suggested by inhibition of anion exchange and interactions with stilbene inhibitor binding (Cobb & Beth, 1990); based on noncompetitive reaction kinetics, a recent analysis of eosin binding to band 3 concluded that lysine 430 may be near but not at the site at which transported anions bind (Liu & Knauf, 1993). Notwithstanding the uncertainty in the precise location of the fluorescent label, the measurements here probe for the first time the rapid dynamics of the intramembrane domain of band 3.

A principal observation was that increasing NaCl concentration significantly accelerated the nanosecond segmental dynamics of the intramembrane domain of band 3, with lesser effect on the rate and extent of fluorescein rotation in its binding pocket. Experiments with a series of small nonionic solutes and multiply charged anions indicated that the effect of NaCl was due to ionic strength, and not to osmolality or anion-specific interactions. Ionic strength did not influence the anisotropy decay of fluorescein-labeled carbonic anhydrase, showing that the ionic strength dependence observed for band 3 was not a nonspecific effect. Further, measurements on ghosts containing trypsin-cleaved band 3 demonstrated that the ionic strength effect required an intact transporter. These results suggest that ionic strength influences the packing of intramembrane helices in band 3 in the vicinity of the fluorescein binding site. Although the major effect occurs at low (subphysiological) ionic strengths, the data provide potentially useful information about band 3 structure. In general, ionic strength influences protein folding by three mechanisms: shielding of electrostatic interactions (Debye−Hückel screening), anion binding to charged sites on the protein (electroselectivity series), and ionic effects on water structure (Hofmeister series) (Goto et al., 1990). For the band 3 studies here, the rate of segmental motion correlated best with Debye length, rather than with the electroselectivity (citrate > sulfate > bromide > chloride > fluoride) or Hofmeister (citrate > sulfate > fluoride > chloride > bromide) series (von Hippel & Schleich, 1969). The charged residues in the relatively polar region of lysine 430 (Lux et al., 1989) are probably involved in these putative electrostatic interactions.

Ginsburg et al. (1981) used an alternative approach to examine band 3 segmental dynamics. Band 3 was conjugated with the spin-label *N*-(1-oxy-2,2,6,6-tetramethyl-4-piperidinyl)maleimide for measurement of probe mobility by electron spin resonance (ESR). Both mobile and immobile components of probe motion were identified, with the mobile fraction increasing with increasing anion concentration. Similar to the fluorescence data here, the fraction of mobile spin probe exhibited half-saturation at low Cl^- concentration (~10 mM). Although direct comparison between data obtained by the two very different methodologies cannot be made, the ESR results are in general agreement with our observation that band 3 segmental motion increases (decreasing τ_{1c}) with increasing anion concentration.

Possible "communication" between segmental dynamics in the intramembrane domain of band 3 and the external sugar moiety or the cytoplasmic domain was examined. Band 3 is heterogeneously glycosylated at a single residue, Asn 642. WGA lectin binding to the sugar moiety did not affect fluorescein motion in the intramembrane domain of band 3, consistent with the observation that endoglycosidase digestion of the sugar on band 3 did not affect band 3 function (Casey et al., 1992). Similarly, changes in the conformation of cdb3 induced by increasing pH in the range 8−10 (Low et al., 1988) and 2,3-DPG binding (Moriyama et al., 1993) had little effect on the fluorescence anisotropy decay. These results are consistent with the finding that cleavage of cdb3 does not affect band 3-mediated anion transport (Lepke et al., 1992), and support the functional independence of the intramembrane domain of band 3.

Do the nanosecond band 3 segmental dynamics probed here correlate with rate-limiting conformational changes that accompany anion exchange? Because the anion exchange turnover rate is rapid (~10^5 s^{-1}), it has been proposed that conformational changes occur in the region of the anion binding domain on the time scale of 10 μs and shorter. There is inadequate structural information on band 3 to specify the nature and molecular location of these conformational changes. As is the case for anion exchange, the segmental motion studied here was not sensitive to maneuvers which affect the external sugar moiety or the internal cytoplasmic domain. However, there are several remarkable differences: (a) anion exchange is strongly temperature-dependent (Brahm, 1977), where the segmental motion studied here was weakly temperature-dependent; (b) anion exchange is pH dependent in the range 5−6.5 (Jennings, 1989), whereas the segmental motion was not. The *rate-limiting* motion of band 3 involved in anion exchange is therefore not the nanosecond segmental motion characterized in these studies. This conclusion is consistent with the proposal that eosin maleimide inhibits anion exchange by locking band 3 in its outward-facing conformation (Liu & Knauf, 1993).

Although the experiments here provide the first time-resolved information on rapid segmental dynamics of the intramembrane domain of band 3 involved in anion transport, they cannot be interpreted in terms of distinct conformational changes which accompany the transport event. Because band 3 structure has been resolved only to low resolution (Wang et al., 1994), the precise location of the bound chromophore and its geometric relationship with respect to the remainder of the intramembrane domain are not known. Therefore, it is not possible to assign the residues involved in constraining rapid fluorophore rotation and those participating in the nanosecond segmental motion. Because of limitations imposed by the short fluorescence lifetime, it is difficult to resolve segmental motions slower than ~200 ns. Such motions may be important in terms of anion exchange mechanisms, but are not observed in this study, not only because they may be too slow but also because fluorophore binding probably perturbs the native band 3 dynamics associated with anion transport. Further measurements of band 3 segmental dynamics in the nanosecond-to-microsecond time range are indicated utilizing site-specific fluo-

rescent probes which do not affect anion exchange.

REFERENCES

Brahm, J. (1977) *J. Gen. Physiol.* 70, 283−306.

Cabantchik, Z. I., Knauf, P. A., & Rotstein, A. (1978) *Biochim. Biophys. Acta* 515, 239−302.

Calafut, T., Dix, J. A., & Verkman, A. S. (1989) *Biochemistry 28*, 5051−5058.

Casey, J. R., & Reithmeier, R. A. F. (1991) *J. Biol. Chem. 266*, 15726−15737.

Casey, J. R., Pirraglia, C. A., & Reithmeier, R. A. F. (1992) *J. Biol. Chem. 267*, 11940−11948.

Clague, M. J., Harrison, J. P., Morrison, I. E. G., Wyatt, K., & Cherry, R. J. (1990) *Biochemistry 29*, 3898−3904.

Cobb, C. E., & Beth, A. H. (1990) *Biochemistry 29*, 8283−8290.

Forman, S. A., Verkman, A. S., Dix, J. A., & Solomon, A. K. (1982) *Biochim. Biophys. Acta 689*, 531−538.

Fushimi, K., & Verkman, A. S. (1991) *J. Cell Biol. 112*, 719−725.

Ginsburg, H., O'Connor, S. E., & Grisham, C. M. (1981) *Eur. J. Biochem. 114*, 533−538.

Goto, Y., Takahashi, N., & Fink, A. L. (1990) *Biochemistry 29*, 3480−3488.

Jennings, M. L. (1989) *Annu. Rev. Biophys. Biophys. Chem. 18*, 397−430.

Kopito, R. R., & Lodish, H. R. (1985) *Nature 316*, 234−238.

Lakowicz, J. R., Cherek, H., Kusba, J., Gryczynski, I., & Johnson, M. (1993) *J. Fluoresc. 3*, 103−116.

Lepke, S., Becker, A., & Passow, H. (1992) *Biochim. Biophys. Acta 1106*, 13−16.

Liu, S. J., & Knauf, P. A. (1993) *Am. J. Physiol. 264*, C1155−C1164.

Low, P. S., Westfall, M. A., Allen, D. P., & Appell, K. C. (1984) *J. Biol. Chem. 259*, 13070−13076.

Lux, S. E., John, K. M., Kopito, R. R., & Lodish, H. F. (1989) *Proc. Natl. Acad. Sci. U.S.A. 86*, 9089−9093.

Macara, I. G., Kui, S., & Cantley, L. C. (1983) *J. Biol. Chem. 258*, 1785−1792.

Moriyama, R., Lombardo, C. R., Workman, R. F., & Low, P. S. (1993) *J. Biol. Chem. 268*, 10990−10996.

Nigg, E. A., & Cherry, R. J. (1980) *Proc. Natl. Acad. Sci. U.S.A. 77*, 4702−4706.

Passow, H. (1986) *Rev. Physiol. Biochem. Pharmacol. 103*, 61−223.

Rao, A., & Reithmeier, R. A. F. (1979) *J. Biol. Chem. 254*, 6144−6150.

Reithmeier, R. A. F. (1993) *Curr. Opin. Struct. Biol. 3*, 515−523.

Salhany, J. M. (1990) *Erythrocyte band 3 protein*, CRC Press, Boca Raton, FL.

Salhany, J. M., Cordes, K. A., & Schopfer, L. M. (1993) *Biochemistry 32*, 7413−7420.

Schnell, K. F., Besl, E., & Manz, A. (1978) *Pflugers Arch. 375*, 87−95.

Tanner, M. J. A. (1993) *Baillier's Clin. Hematol. 6*, 333−356.

Thevenin, B. J. M., Periasamy, N., Shohet, S. B., & Verkman, A. S. (1994) *Proc. Natl. Acad. Sci. U.S.A. 91*, 1741−1745.

Verkman, A. S., Dix, J. A., & Solomon, A. K. (1983) *J. Gen. Physiol. 81*, 421−449.

von Hippel, P. H., & Schleich, T. (1969) *Biological Macromolecules* (Timasheff, S., & Fasman, G., Eds.) Vol. II, pp 462−466, Marcel Dekker, New York.

Wang, D. N. (1994) *FEBS Lett.* 346, 26−31.

Wang, D. N., Sarabia, V. E., Reithmeier, R. A. F., & Kuhlbrandt, W. (1994) *EMBO J.* 13, 3230−3235.

Yamakose, H., Sato, Y., & Suzuki, Y. (1993). *Biol. Pharm. Bull.* 16, 1282−1287.

BI9504872